ELECTROMAGNETIC LOADS AND STRUCTURAL RESPONSE OF THE CIT VACUUM VESSEL TO PLASMA DISRUPTIONS*

CONF-871007--105

DE89 000646

S. L. Salem, G. Listvinsky, M. Y. Lee, C. Bailey
TRW Inc., One Space Park
Redondo Beach, CA 90278

Abstract

Studies of the electromagnetic loads produced by a variety of plasma disruptions, and the resulting structural effects on the Compact Ignition Tokamak (CIT) vacuum vessel (VV), have been performed to help optimize the VV design. A series of stationary and moving plasmas, with disruption rates from 0.7 - 10.0 MA/ms, have been analyzed using the EMPRES code to compute eddy currents and electromagnetic pressures, and the NASTRAN code to evaluate the structural response of the vacuum vessel. Key factors contributing to the magnitude of EM forces and resulting stresses on the vessel have been found to include disruption rate, and direction and synchronization of plasma motion with the onset of plasma current decay. As a result of these analyses, a number of design changes have been made, and design margins for the present 1.75 meter design have been improved over the original CIT configuration.

Introduction

The Compact Ignition Tokamak (CIT) will be the first U.S. fusion machine designed to study ignited plasmas. One of the major concerns of the CIT Program is the effect of full power plasma disruptions on the vacuum vessel (VV) and internals. Over the design lifetime of 3000 full power pulses, each with a fusion yield of 1.5 GJ, the CIT vessel and all internals are required to withstand a disruption frequency of 10 percent "without significant operational impairment." Therefore, during the design phase, major efforts are being made to assess the magnitudes of electromagnetic loads acting on the CIT vacuum vessel from a variety of plasma disruption events, and to evaluate the impact of these loads on the vessel.

The present CIT vacuum vessel (Figure 1), is designed for a plasma with a 1.753 meter major radius, capable of operating in double and single null divertor configurations, and in a limiter mode. Table 1 lists key plasma parameters of the device. The VV shell will have single wall construction, and the VV coolant channels will be welded to the wall. The VV wall and internals will be cooled between pulses by GN2. The VV wall will be made of 3 cm thick Inconel 625, with an additional 1 cm allocated for the coolant channels. If necessary, the VV buckling stiffness can be further increased, and bending stress in the wall can be reduced by using double wall construction and locating the coolant channels between the walls.

Table 1. CIT Plasma Parameters

Major Radius	1.753 m
Minor Radius	0.55 m
Elongation	1.8 - 2.0
Triangularity	> 0.3
Plasma Current	9 MA
Full Current Plasma Flat Top	5 sec
Fusion Yield	1.5 GJ
Toroidal field (on axis)	10 T

This paper will report on the results of analyses performed during 1987 on recent CIT VV designs, which continue earlier studies on previous designs. [1] For

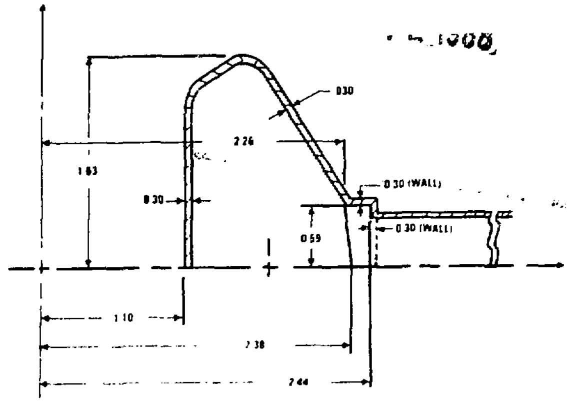

Figure 1. CIT R_o = 1.75m Single Wall Vacuum Vessel

these analyses, the computer code EMPRES (ElectroMagnetic PREssure in Shells) was used to compute the eddy currents and electromagnetic pressures resulting from specified plasma disruptions. A 180 degree NASTRAN finite element model was then constructed to analyze the resulting static and buckling behavior, and to compute vibratory frequencies and modes of the vessel. Four moving plasma disruptions were analyzed, using plasma motions and currents generated by R. Sayer of FEDC with the PPPL Tokamak Simulation Code (TSC). These cases are summarized in Table 2.

Table 2. Moving Plasma Disruptions for CIT VV Analysis

Case	Plasma Motion	Disruption Rate
1	Inboard horizontal	-2.6 MA/ms
2	Inboard horizontal	-0.7 MA/ms
3	Vertical	-2.6 MA/ms
4	Vertical	-0.7 MA/ms

The objectives of this work were to verify space allocation for the VV wall and coolant channels, to check the necessity of double wall construction, to determine loads acting on the VV supports, and to establish further analysis requirements.

The analyses performed to date show that the present 1.75 meter VV has safety margins higher than those for the earlier designs.

Electromagnetic Analysis

Model

The VV model (Upper half) used for the electromagnetic analyses is shown in Figure 2. The model consists of 48 axisymmetric, curvilinear plates. Each plate is defined by two endpoints and a central node. For these axisymmetric analyses, current flows only in the toroidal direction, and is calculated at the central node of each plate. Once the eddy currents through each plate of the VV have been calculated, EM pressures are then computed from the magnetic fields and electric currents. For the EM analysis, the region of the 16 horizontal ports was simulated by increasing the resistivity of the Inconel by a factor of two. Loads on the port plates were assessed in additional EMPRES runs that modeled these elements explicitly.

*Research sponsored by the Office of Fusion Energy, U.S. Department of Energy, under contract number 41Y-56517C, with Martin Marietta Energy Systems, Inc.

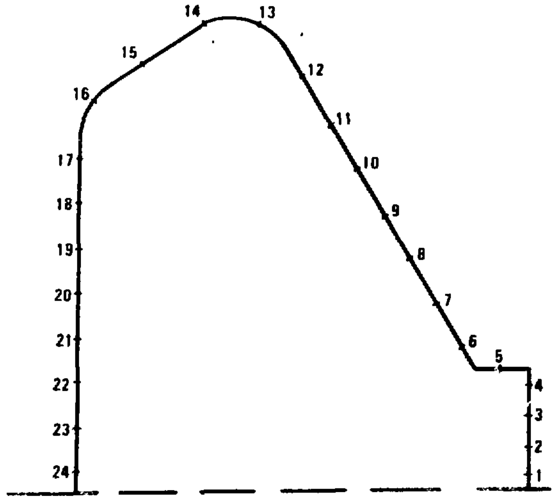

Figure 2 CIT Vacuum Vessel, EM Model, Upper Half

In the EM analysis, the PF and OH coils, as well as the plasma itself, are modeled as time-varying filamentary current sources. For the 1.75 meter VV analyses, it was assumed that the PF and OH coil currents remained constant throughout the disruption events. This is considered a somewhat conservative assumption, since coupling to the coils during the course of a disruption is expected to reduce coil currents by up to 20 percent. Our previous analyses indicated peak pressure reductions of 12 to 18 percent as a result of this effect.

The plasma was modeled as a set of nine filaments (coils), whose currents were changing during the course of a disruption. Each filament carried one-ninth of the total current at any time, and the filament locations were changed with each time step to represent the motion and collapse of the plasma. Such a plasma model had previously produced 30 percent more accurate results in comparisons with single filament models for stationary disruptions; such a difference would be accentuated for moving plasma disruptions as the plasma approached the vessel wall.

Analysis Results

Three different types of plasma disruptions have been investigated to date: stationary, plasma moving horizontally inboard while disrupting, and loss of vertical stability (downward motion) followed by disruption. The stationary disruptions were run first, with earlier VV geometries, to investigate the effects of disruption rate on vessel loads. During the course of these analyses, a post-processor code was written to take the output of the TSC code and generate the plasma filament locations and current magnitudes for the EMPRES input; a second code was written to translate the EMPRES EM pressure output into the forces required for the NASTRAN analyses.

Earlier studies had shown that the interactions of plasma motions with plasma current decay rates would play a significant role in determining the peak VV loads. Thus the early set of runs was performed to investigate the effects of plasma current decay rates in the absence of plasma motion. Figure 3 shows the peak inboard and outboard normal pressures for current decays in the range of -1 to -10 MA/ms. These studies were performed for an earlier, similar design with Ro = 1.60 m and 3 cm VV wall thickness. It is apparent that, for this particular geometry, the peak pressures are most sensitive to rates up to 1 MA/ms, whereas an

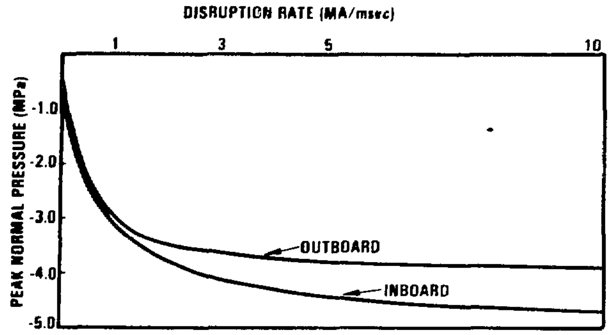

Figure 3. Peak Normal Pressure vs. Disruption Rate for Stationary Disruption, R_0 = 1.60 m

increase in disruption rate above 3 MA/ms has little effect upon the peak pressures; of course, the dynamic behavior of the vessel may still depend upon the rate. The 1 and 3 MA/ms rates correspond approximately to the CIT design categorization of disruptions as "ordinary" (about 0.7 - 1.0 MA/ms), and "extraordinary" (about 2.7 - 3.0 MA/ms), with the expectation that about 10 percent of the total disruptions would fall into the "extraordinary" range.

Following these stationary disruptions, the four moving plasmas listed in Table 2 were analyzed for the 1.75 m geometry, and the most significant load distributions were used to perform static and buckling analyses with NASTRAN. Figures 4-6, from Case 1, (plasma motion towards inboard wall), illustrate the general aspects of the important EM effects in all four cases. In the driving plasma, significant inward plasma motion preceded the onset of the peak plasma current decay (at 0.5 ms), after which plasma decay dominated. Figure 4 illustrates that EM pressures follow the direction of plasma motion (away from plasma on the inboard wall, towards plasma on the outboard wall), and then all pressures become inward towards the plasma once plasma disruption begins. Figure 5 shows the distribution of pressures around the vessel at the peak of plasma motion (0.4 ms), and Figure 6 shows them at the point of peak pressure during plasma current decay. These clearly show the asymmetric pressures during plasma motion, and the more symmetric pressures induced by plasma current decay. It should be emphasized that only normal pressure on the VV is shown in Figures 4 - 7; however, both normal and tangential pressure components were computed and both were used in the structural analysis.

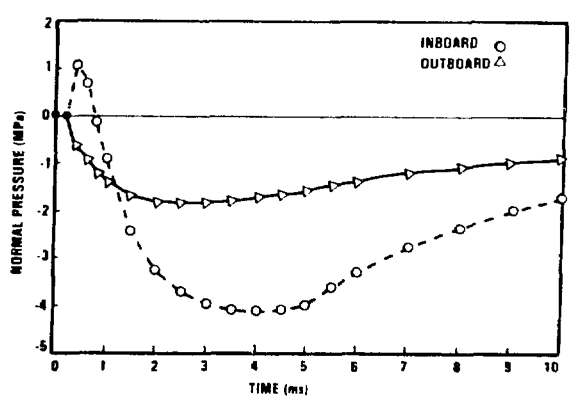

Figure 4. Normal Pressure Time History, Inboard Plasma Motion, Extraordinary Disruption

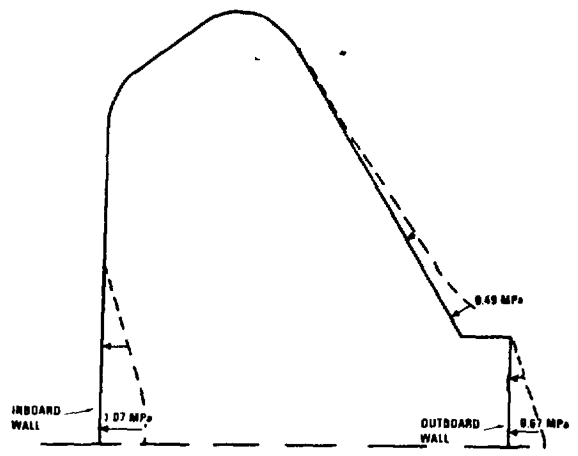

Figure 5. Normal Pressure Distribution, Inboard Plasma Motion, Extraordinary, 0.4 msec

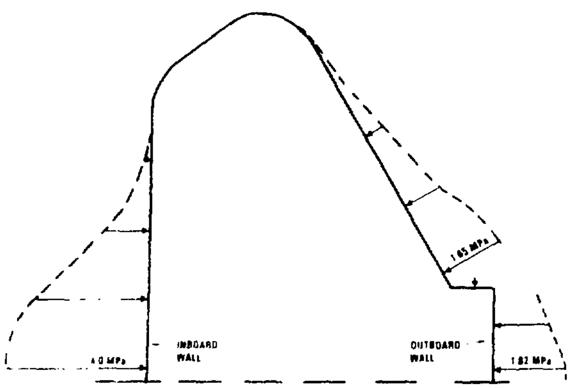

Figure 6. Normal Pressure Distribution, Inboard Plasma Motion, Extraordinary, 3.0 ms

The change of pressure direction on the inboard wall indicates the importance of the exact timing of plasma motion and disruption, since the magnitude and direction of the peak forces depend upon the amount of initial motion, the closeness of the plasma to the near wall at the time of peak current decay, and the amount of VV eddy current reversal induced by the ultimate disruption. The case of vertical plasma motion results in a net vertical force on the VV, which determines the forces on the VV supports and the extent of vertical VV motion Figure 7 shows VV pressures during vertical plasma motion (case 4), with the plasma nearing the bottom. At this point, a net downward force, in addition to local pressures in the vicinity of the moving plasma, are present.

Structural Analysis

For the present structural analyses, a 180 degree NASTRAN finite element model was constructed for the VV and ports, as shown in Figure 8. The model was formed by CQUAD4 isoparametric quadrilateral shell elements; symmetry boundary conditions were used at 0 and 180 degree planes. Constraints in the vertical and toroidal directions were provided at the middle of the ports.

Five spatial load distributions were selected as input for NASTRAN structural analyses. These cases are summarized in Table 3. The selected load distributions represent expected worst cases in terms of static stress, buckling safety factors of both the inboard and outboard walls, and vertical displacement in the VV.

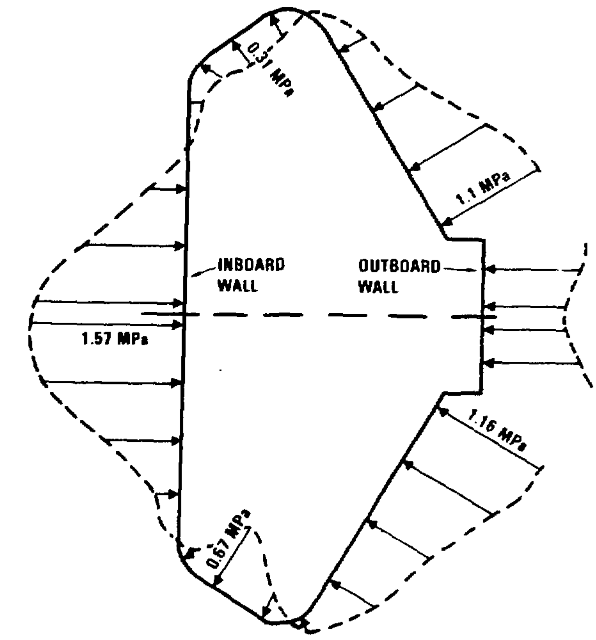

Figure 7. Normal Pressure Distribution, Downward Plasma Motion, Ordinary Disruption, 14 ms

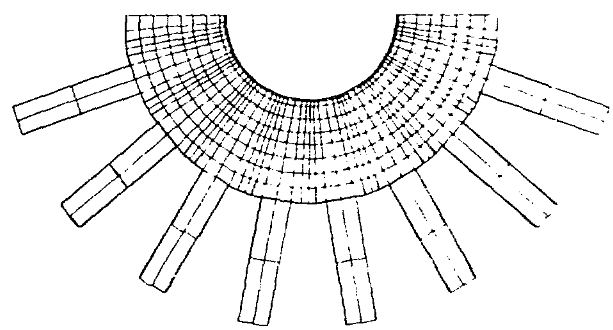

Figure 8. Finite Element Vacuum Vessel Model

Note that the "ordinary" vertical disruption case produced significantly higher net vertical force than the "extraordinary", whereas the "extraordinary" inboard moving plasma disruption produced slightly higher loads than the respective "ordinary" case

Table 3. Load Case Summary

Case		Load Description
1	Inboard moving, Extraordinary	τ = 3.0 msec (see Figure 6) Possibility of outboard buckling
2	Inboard moving, Extraordinary	τ = 0.4 msec (see Figure 5) Possibility of inboard buckling
3	Vertical motion, Extraordinary	τ = 3.6 msec (at point of max net vertical force: 3200 kNt) Pressure dist. similar to case 1
4	Vertical motion, Ordinary	τ = 7.4 msec; net vertical force = 3800 kNt. Pressure dist. different from case 1.
5	Vertical motion, Ordinary	τ = 14.0 msec (at point of max net vertical force: 9300 kNt)

In addition to the above cases, a uniform (vacuum) pressure case (case 6) was analyzed, and vibratory frequencies and modes of the VV were calculated. A summary of the analysis results is given in Table 4, showing the buckling safety factors (BSF), maximum membrane stress in the inboard and outboard walls, and the maximum vertical displacements in the VV shell. The VV inboard buckling mode is shown in Figure 9, and VV static deformations under a 9300 kNt vertical force (case 5) are shown in Figure 10.

Table 4. Structural Analysis Summary

Case	Buckling Safety Factor (BSF)	Membrane Stress(MPa) Inboard	Membrane Stress(MPa) Outboard	Vertical Displ.
1	14.4 (Outboard)	145	-150	
2	14.0 (Inboard)	-48	50	
[illegible]	Similar to case 1	160	-150	0.29 cm
[illegible]	Similar to case 1	160	-150	0.30 cm
[illegible]		55	-180	0.86 cm
6	127. (Outboard)	4	-10	

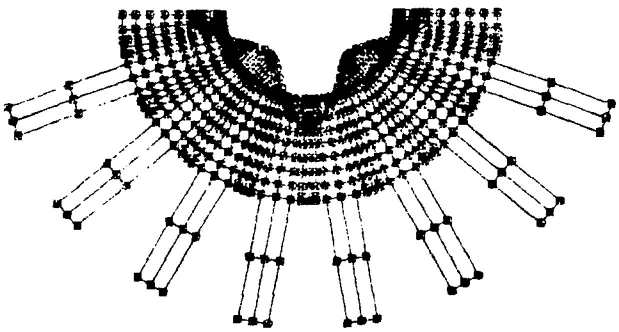

Figure 9. Vacuum Vessel Inboard Buckling Mode

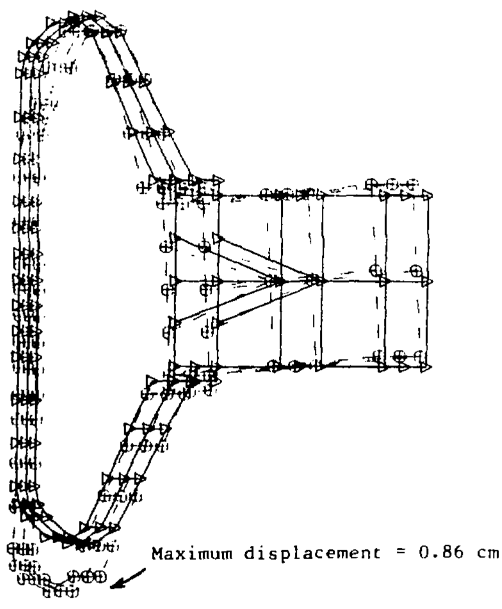

Figure 10. VV Static Deformation at Fvert = 9300 kNt

More detailed analysis of the results showed that the location and direction of the VV maximum stress is a strong function of plasma disruption scenario. For example, for cases 1, 2 and 3, the maximum stress is toroidal inboard stress near the machine midplane, whereas for case 5, maximum stress is poloidal near the vessel top and bottom. The results presented in Table 4 indicate that the elastic buckling is of low importance for the CIT vacuum vessel. Significant plastic deformation of the VV will take place prior to buckling. Hence, the predicted VV critical failure mode is overstressing (excessive local plastic deformation and/or crack propagation); more detailed analysis of stress distribution near the ports is necessary. For the present VV support system, the reaction loads are non-uniformly distributed. The reaction loads on supports located near the 0 and 180 degree planes are approximately 50 percent higher than loads on supports further from these planes. The VV fundamental frequency in the vertical direction equals 52.5 Hz, and the respective vibratory mode is similar to the deflection shape shown in Figure 10.

For the loads analyzed, the VV space allocation is adequate and 3 cm single wall construction is sufficient if the dynamic amplification factor (DAF) ≤ 1.5, and the ASME B&PV Code design allowables are used for Inconel 625, with a yield stress of about 415 MPa.

Conclusions

The analysis performed shows that, as designed, the CIT vacuum vessel has a static safety factor of 1.5 and a high buckling safety factor for the analyzed disruption scenarios. Since the plasma disruption loads are dynamic in nature and the DAF can theoretically equal 2.0, a dynamic time history analysis for the VV must be performed to verify the design.

It was found that the EM forces acting on the VV wall during plasma disruptions are very sensitive to synchronization of plasma motion with the onset of current decay in the plasma, as well as to the direction of plasma motion. Hence, additional studies of other plasma disruption scenarios will be necessary to verify the VV design load envelope.

References

[1] G. Listvinsky, J.J. Weede, S.L. Salem, A. Wolfson, "First Wall and Vacuum Vessel Analysis for Compact Ignition Tokamaks," Fusion Technology, vol 10, pp. 514-520, November 1986.

DISCLAIMER